Excel Approach for Infiltration Capacity for Different Lands

Alaa Nabil El-Hazek[1*]

[1]*Department of Civil Engineering, Faculty of Engineering at Shoubra, Benha University, Shoubra 11689, Cairo, Egypt.*

Author's contribution

The sole author designed, analyzed, interpreted and prepared the manuscript.

Original Research Article	*Received 15 August 2018* *Accepted 13 October 2018* *Published 23 October 2018*

ABSTRACT

This paper presents an Excel approach for infiltration capacity for different types of lands. That is to employ the popular Microsoft Excel software to represent the measured infiltration data graphically. Regression analysis is performed for the accumulated infiltration versus the time. Equations are obtained to predict the accumulated infiltration at required times.

Thirty one raw infiltration measurements from various sources are gathered, studied and analyzed applying this approach. Measurements include different types of soil textures and land covers. The infiltration rates are measured by the commonly used infiltrometer. Both single infiltrometer and double infiltrometer are employed.

It is concluded that the presented Polynomial infiltration model of Excel approach for the accumulated infiltration is associated with high accuracy, where the values of coefficient of determination (R^2) range between 0.9850 and 0.9998. The obtained equations can help in irrigation processes.

All the gathered raw experimental infiltration measurements are also analyzed employing Horton and Kostiakov infiltration models. It is found that the Polynomial infiltration model of Excel approach has higher accuracy, followed by Kostiakov model, and finally Horton model. The values of different constants of Horton and Kostiakov infiltration models for all cases are obtained. The accuracy of the Polynomial, Horton and Kostiakov infiltration models are studied considering the types of soil texture and land cover.

_____

Corresponding author: Email: alaa_elhazek@yahoo.com;

Investigating the constants A, B and C of the obtained equation of the polynomial infiltration model of Excel approach, it is found that all A values are negative, all B values are positive, and all C values are positive except for sandy clay and sandy clay loam soils. There is no specific trend for the effect of the associated land cover on constants A, B, and C except for loamy sand soil, where B and C values for bare land are greater than their values for irrigated land.

1. INTRODUCTION

Infiltration occurs when water on the land surface enters into the soil. Infiltration rate is the rate at which soil is able to absorb rainfall or irrigation water. It decreases as the soil becomes saturated. When the precipitation rate exceeds the infiltration rate, runoff will occur. It is related to the saturated hydraulic conductivity of the near-surface soil.

The process of infiltration continues when there are spaces for additional water at the soil surface. The available volume for additional water in the soil depends on the porosity of the soil. The infiltration capacity is the maximum rate that water can enter a soil in a given condition.

There are several methods to predict the rate of infiltration. For uniform initial soil water content and a deep well-drained soil, there are some approximate methods to solve for the infiltration such as the Green and Ampt method [1] and [2]. It is a function of the soil suction head, porosity, hydraulic conductivity and time. There are also empirical methods such as Horton and Kostiakov methods.

Horton method [2] and [3] suggested that infiltration capacity declines rapidly and tends towards an approximately constant value. It is an empirical formula showing that infiltration starts at some value and is decreasing exponentially with time. After some time when the soil saturation level reaches a certain value, the rate of infiltration tends to a constant rate.

Kostiakov method [4] includes an empirical equation assuming that the intake rate declines over time according to a power function. The major limitation of the equation is its reliance on the zero final intake rates. In most cases, the infiltration rate instead approaches a finite steady value, which in some cases may occur after short periods of time.

The Kostiakov-Lewis method [5], also known as the "Modified Kostiakov" equation, corrects for this by adding a steady intake term to the original equation.

The rate of infiltration is often measured in millimeters per hour or inches per hour. It can be measured using an instrument that called infiltrometer. The common double infiltrometer, [6] and [7], is shown in Fig. 1 with falling head and constant head arrangements. There is also a single infiltrometer, [8] and [9], which is illustrated in Fig. 2.
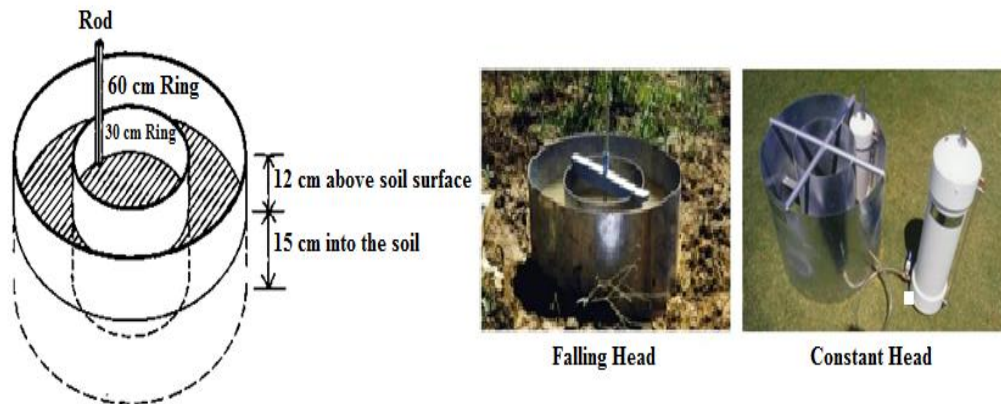
Fig. 1. Double infiltrometer, [6] and [7]
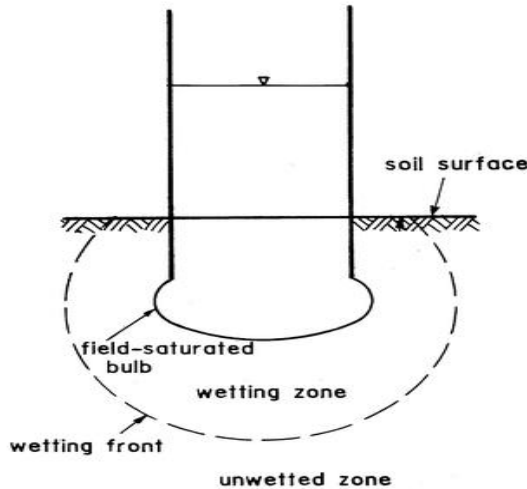
Fig. 2. Single infiltrometer, [8] and [9]

The infiltration rate is affected by soil characteristics including the soil texture and structure, water content of the soil, and types of land cover. Many researches are done to investigate the effect of these parameters on the infiltration rate. For example, effect of specific grazing land conservation practices on watershed processes is necessary for future planning and resource allocation, [10]. Also, vegetation and/or better land management can prevent soil from drying out quickly, which is important in agriculture and irrigation practices, [11].

An Excel approach for infiltration capacity for different types of soils and land covers is introduced. That is to employ the popular Microsoft Excel software to represent the measured infiltration data graphically. The accumulated infiltration is plotted versus the time. Polynomial regression analysis is performed for the accumulated infiltration against the time. Equations are obtained easily to predict the accumulated infiltration. The introduced polynomial infiltration model of Excel approach for the accumulated infiltration has higher accuracy than the widely used Horton and Kostiakov infiltration models.

2. MATERIALS AND METHODS

An Excel approach for infiltration capacity for different types of soils is introduced. That is to employ the popular Microsoft Excel software to represent the measured infiltration data graphically. The accumulated infiltration is plotted

versus the time. Regression analysis is performed for the accumulated infiltration against the time. Equations are obtained to predict the accumulated infiltration at required times. The obtained equations can help in irrigation processes. It is possible to determine how long it will take to infiltrate a certain amount of water, which is important to determine the irrigation time and quantity.

Thirty one raw infiltration measurements from various sources are gathered, studied and analyzed applying this approach. Raw infiltration measurements include various locations with different types of soil textures and land covers. The studied infiltration rates are measured by the commonly used infiltrometer. Both single infiltrometer and double ring infiltrometer are used for these measurements.

All the gathered raw experimental infiltration measurements are also analyzed employing both Horton and Kostiakov infiltration models. The values of different constants of Horton and Kostiakov infiltration models for all cases are obtained.

3. RESULTS AND DISCUSSION

3.1 Polynomial Infiltration Model of Excel Approach

All the gathered thirty one raw infiltration measurements from various sources represent field tests. In dry soil, water infiltrates rapidly, which is called the initial infiltration rate. As more water replaces the air in the pores, the water

from the soil surface infiltrates more slowly and eventually reaches a steady rate, which is called the basic infiltration rate, [6]. It is recommended that at least two infiltration tests should be carried out at a site to make sure that the correct results are obtained. Also, the infiltration curve should be determined for normal soil moisture conditions before irrigation takes place (usually when the top soil is dry) [6].

Experimental infiltration measurements are carried out at an irrigated farm, [6], with loam soil using a double ring infiltrometer with inside diameter of 30 cm and outside diameter of 60 cm, as shown in Table 1. Excel approach is applied on the raw infiltration data, where Fig. 3 illustrates the accumulated infiltration versus the time, a polynomial regression, and the obtained equation with a very high coefficient of determination (R^2). For the obtained equation; AI is the acc. (accumulated) infiltration in mm, and T is the time in min. (minutes).

Excel approach is applied on another experimental infiltration measurements that are carried out at an irrigated land, [12], with sandy clay loam soil using a double ring infiltrometer with diameters of 30 cm and 60 cm. Raw infiltration data are shown in Table 2, while Fig. 4 illustrates the accumulated infiltration versus the time, the polynomial regression, and the obtained equation with a very high R^2.

Using a double ring infiltrometer with diameters of 30 cm and 60 cm, experimental infiltration measurements are performed at ten locations in

two different agricultural lands [13]. Soil texture analyses and land covers are shown in Table 3. The raw infiltration data for the accumulated infiltration are presented in Tables 4 and 5. Applying Excel approach, Figs. 5 and 6 illustrate the accumulated infiltration versus the time, the polynomial regression, and the obtained equations with very high R^2.

Table 1. Raw measurements, [6], for infiltration in loamy irrigated farm with a double ring infiltrometer

Time, min	Accumulated Infiltration, mm
2	8
5	15
10	25
20	42
30	53
40	60
60	69

Table 2. Raw measurements, [12], for infiltration in sandy clay loam irrigated land with a double ring infiltrometer

Time, min	Accumulated Infiltration, mm
1.0	14
1.5	24
2.0	33
2.5	40
3.0	46
3.5	52
4.0	58
4.5	63
5.0	68

$$AI = -0.0182T^2 + 2.1559T + 4.6878$$
$$R^2 = 0.9979$$
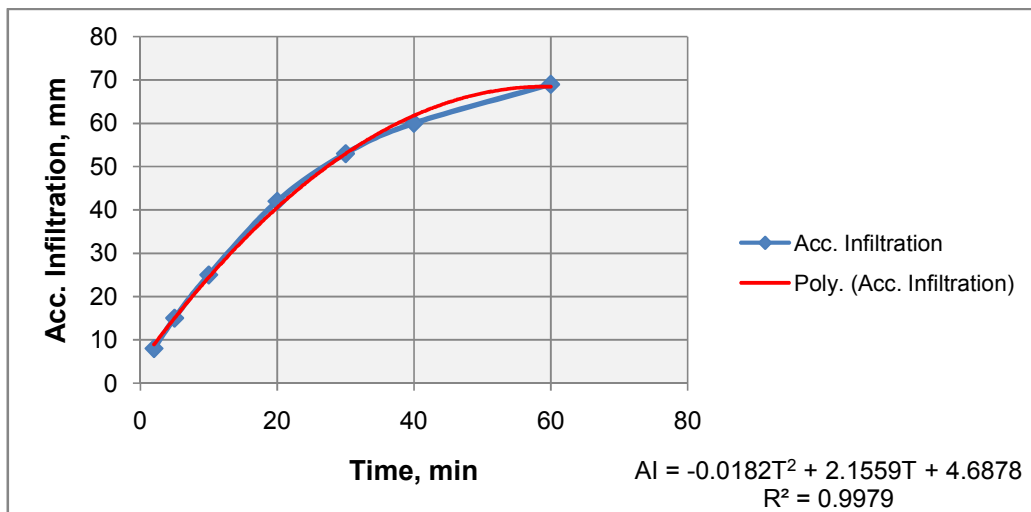
Fig. 3. Accumulated infiltration and the obtained equation in loamy irrigated farm

$$AI = -1.329T^2 + 21.141T - 5.0238$$
$$R^2 = 0.9988$$

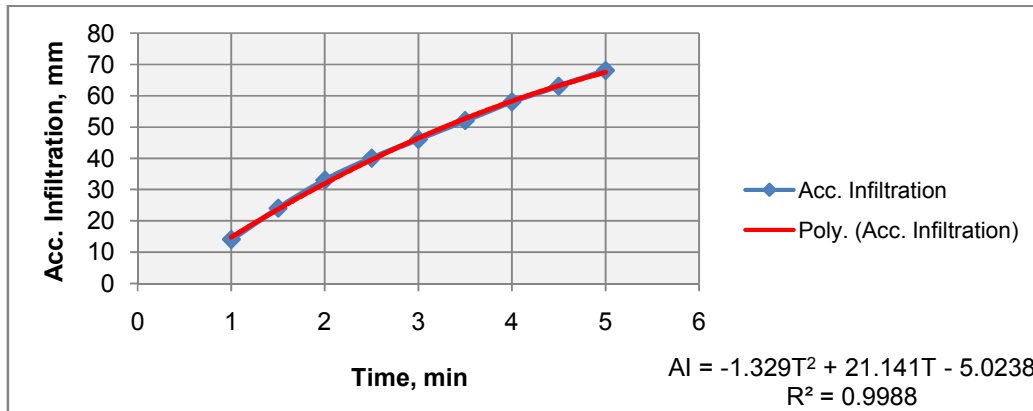**Fig. 4. Accumulated infiltration and the obtained equation in sandy clay loam irrigated land**

Table 3. Soil texture analysis [13], and land covers for two different agricultural lands

Location	land cover	% Sand	% Silt	% Clay	Soil Texture
A 1	Bare land	64	23	13	Sandy Loam
A 2	Bare land	69	18	13	Sandy Loam
A 3	Bare land	55	25	20	Sandy Clay Loam
A 4	Vegetation land	74	15	11	Sandy Loam
A 5	Vegetation land	71	20	9	Sandy Loam
B 1	Bare land	71	20	9	Sandy Loam
B 2	Bare land	77	16	7	Loamy Sand
B 3	Bare land	79	14	7	Loamy Sand
B 4	Vegetation land	51	32	17	Loam
B 5	Vegetation land	56	30	14	Sandy Loam

Table 4. Raw measurements [13], for infiltration in the first agricultural land

Location Time, min	A 1 Acc. Infiltration - A1, mm	A 2 Acc. Infiltration - A2, mm	A 3 Acc. Infiltration – A3, mm	A 4 Acc. Infiltration – A4, mm	A 5 Acc. Infiltration – A5, mm
5	19	24	24	28	26
10	26	33	45	37	50
15	30	37	63	44	65
20	33	39	69	47	76
25	36	41	75	50	87

Table 5. Raw measurements [13], for infiltration in the second agricultural land

Location Time, min	B 1 Acc. Infiltration - B1, mm	B 2 Acc. Infiltration - B2, mm	B 3 Acc. Infiltration – B3, mm	B 4 Acc. Infiltration – B4, mm	B 5 Acc. Infiltration – B5, mm
5	61	86	50	51	95
10	109	139	79	90	172
15	150	183	101	117	240
20	186	221	126	140	280
25	208	250	147	154	317
30	229	277	166	167	349
35	250	304	185	180	381
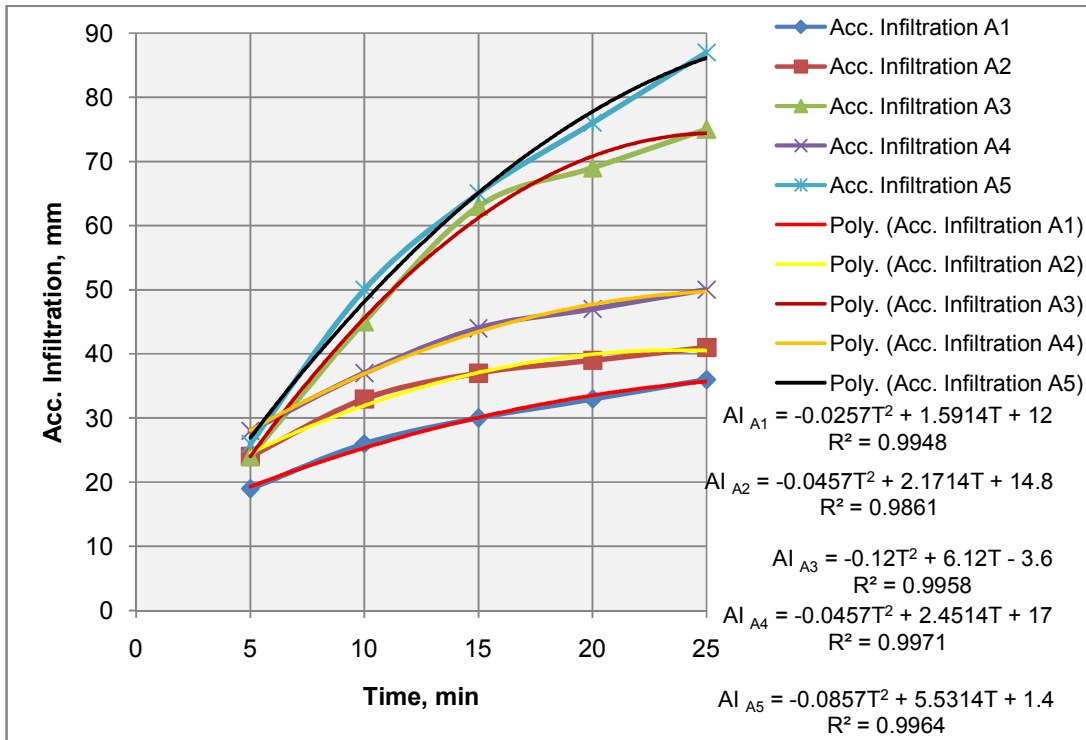
Fig. 5. Accumulated infiltration and the obtained equations for the first agricultural land

The equations shown in Fig. 5:

$$AI_{A1} = -0.0257T^2 + 1.5914T + 12$$
$$R^2 = 0.9948$$

$$AI_{A2} = -0.0457T^2 + 2.1714T + 14.8$$
$$R^2 = 0.9861$$

$$AI_{A3} = -0.12T^2 + 6.12T - 3.6$$
$$R^2 = 0.9958$$

$$AI_{A4} = -0.0457T^2 + 2.4514T + 17$$
$$R^2 = 0.9971$$

$$AI_{A5} = -0.0857T^2 + 5.5314T + 1.4$$
$$R^2 = 0.9964$$
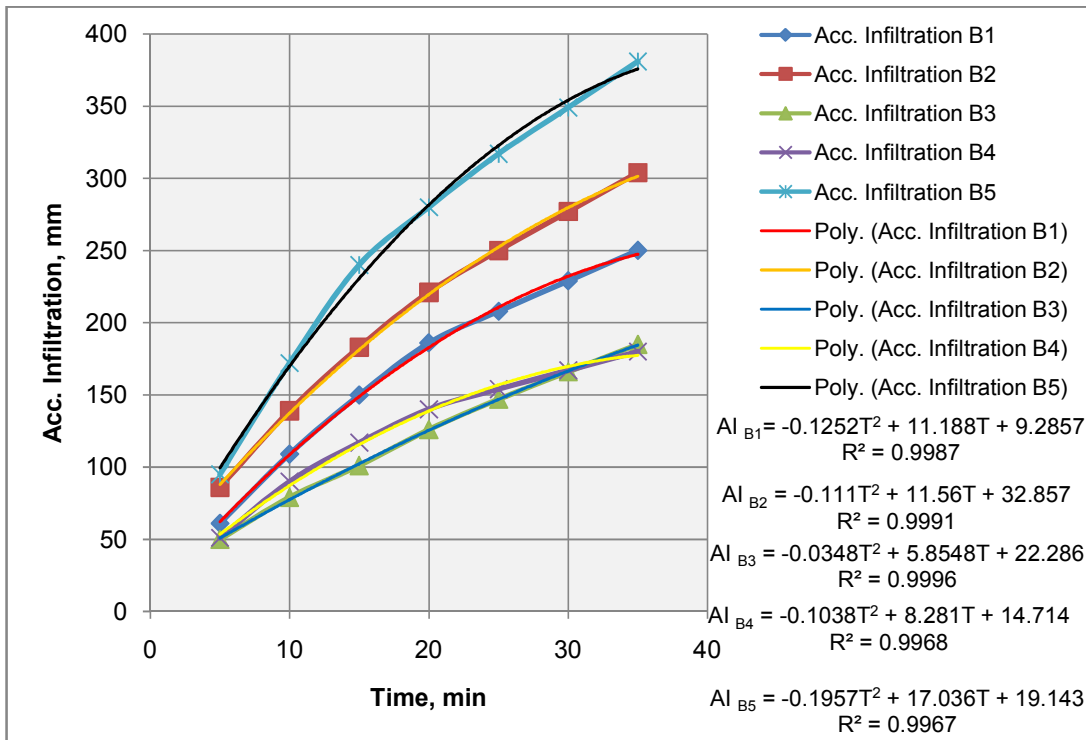
Fig. 6. Accumulated infiltration and the obtained equations for second agricultural land

The equations shown in Fig. 6:

$$AI_{B1} = -0.1252T^2 + 11.188T + 9.2857$$
$$R^2 = 0.9987$$

$$AI_{B2} = -0.111T^2 + 11.56T + 32.857$$
$$R^2 = 0.9991$$

$$AI_{B3} = -0.0348T^2 + 5.8548T + 22.286$$
$$R^2 = 0.9996$$

$$AI_{B4} = -0.1038T^2 + 8.281T + 14.714$$
$$R^2 = 0.9968$$

$$AI_{B5} = -0.1957T^2 + 17.036T + 19.143$$
$$R^2 = 0.9967$$

Employing a double ring infiltrometer with diameters of 45 cm and 60 cm, experimental infiltration measurements are executed three different times for a forest land, [14], as shown in Table 6. Excel approach is applied on the raw infiltration data, where Fig. 7 illustrates the accumulated infiltration versus the time, the polynomial regression, and the obtained equations with very high R^2.
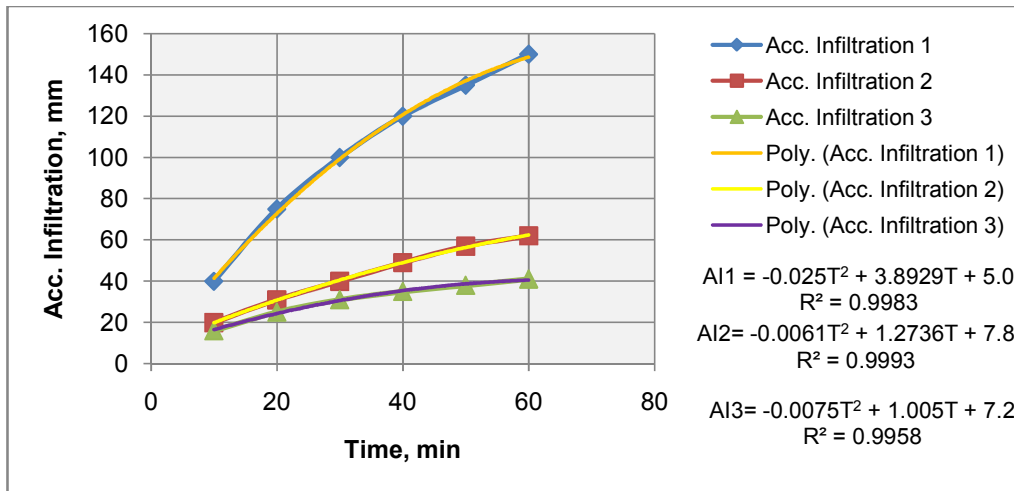
A single infiltrometer is employed to get experimental measurements for infiltration rates in a forest land [14]. A single infiltrometer with 15 cm diameter obtained the infiltration measurements shown in Table 7, and another single infiltrometer with 30 cm diameter gave the infiltration measurements shown in Table 8. Excel approach is applied on the raw infiltration data as illustrated in figures 8 and 9 respectively.

Employing a double ring infiltrometer with diameters of 30 cm and 60 cm, experimental infiltration measurements are carried out for two types of soil textures, [15], which are shown in Table 9. Applying Excel approach on the raw infiltration data shown in Table 10, Fig. 10 illustrates the accumulated infiltrations versus the time, the polynomial regressions, and the obtained equations with very high R^2.

Table 6. Raw measurements, [14], for infiltration in a forest land with a double ring infiltrometer

Time, min	Experiment 1 Acc. Infiltration 1, mm	Experiment 2 Acc. Infiltration 2, mm	Experiment 3 Acc. Infiltration 3, mm
10	40	20	16
20	75	31	25
30	100	40	31
40	120	49	35
50	135	57	38
60	150	62	41

Poly. (Acc. Infiltration 1)
Poly. (Acc. Infiltration 2)
Poly. (Acc. Infiltration 3)

$AI1 = -0.025T^2 + 3.8929T + 5.0$
$R^2 = 0.9983$
$AI2 = -0.0061T^2 + 1.2736T + 7.8$
$R^2 = 0.9993$
$AI3 = -0.0075T^2 + 1.005T + 7.2$
$R^2 = 0.9958$

Fig. 7. Accumulated infiltration and the obtained equation for a forest land
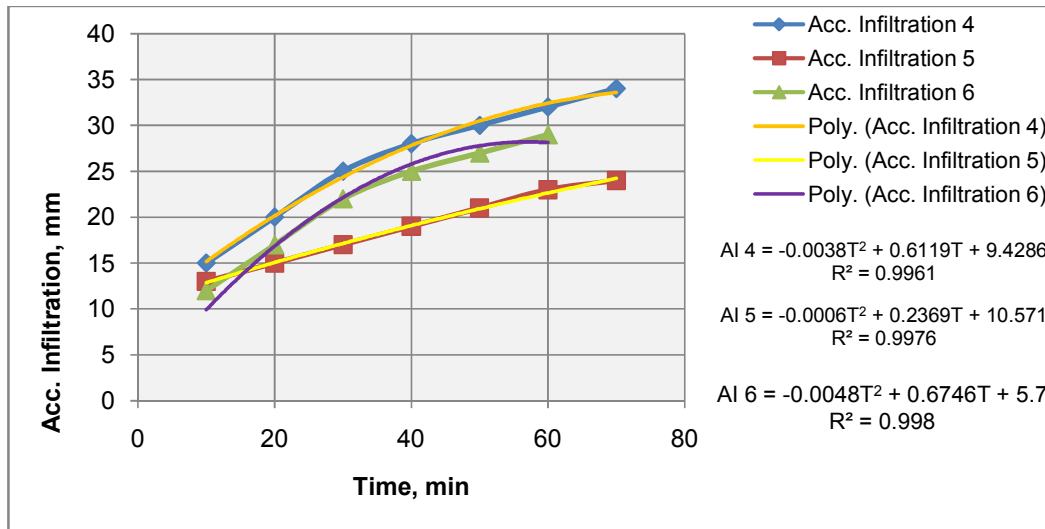
Table 7. Raw measurements, [14], for infiltration in a forest land with 15 cm diameter single ring infiltrometer

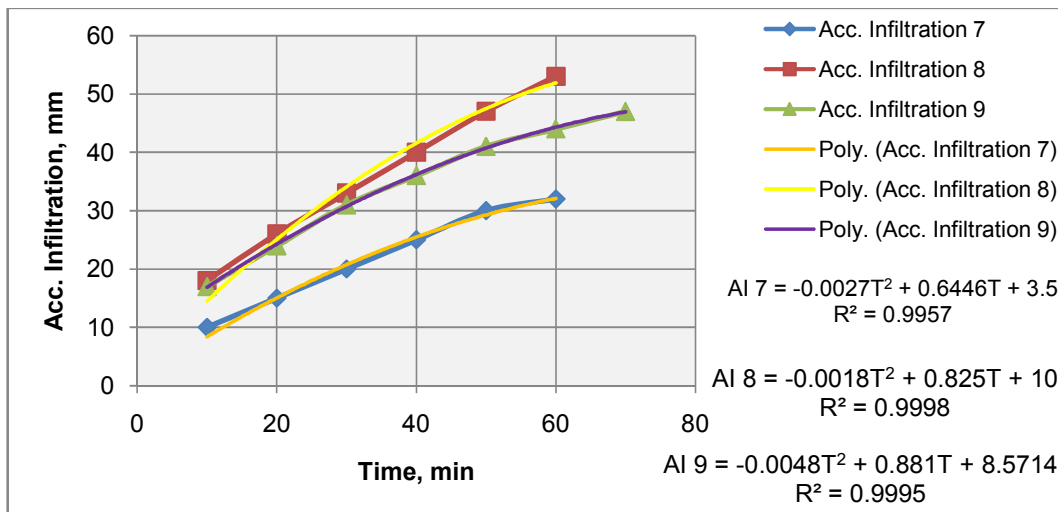| Time, min	Experiment 4 Acc. Infiltration 4, mm	Experiment 5 Acc. Infiltration 5, mm	Experiment 6 Acc. Infiltration 6, mm
10	15	13	12
20	20	15	17
30	25	17	22
40	28	19	25
50	30	21	27
60	32	23	29
70	34	24	---

7

Table 8. Raw measurements, [14], for infiltration in a forest land with 30 cm diameter single ring infiltrometer

Time, min	Experiment 7	Experiment 8	Experiment 9
	Acc. Infiltration 7, mm	Acc. Infiltration 8, mm	Acc. Infiltration 9, mm
10	10	18	17
20	15	26	24
30	20	33	31
40	25	40	36
50	30	47	41
60	32	53	44
70	---	---	47

$AI\ 4 = -0.0038T^2 + 0.6119T + 9.4286$
$R^2 = 0.9961$

$AI\ 5 = -0.0006T^2 + 0.2369T + 10.571$
$R^2 = 0.9976$

$AI\ 6 = -0.0048T^2 + 0.6746T + 5.7$
$R^2 = 0.998$

Fig. 8. Accumulated infiltration and the obtained equation using 15 cm diameter single infiltrometer

$AI\ 7 = -0.0027T^2 + 0.6446T + 3.5$
$R^2 = 0.9957$

$AI\ 8 = -0.0018T^2 + 0.825T + 10$
$R^2 = 0.9998$

$AI\ 9 = -0.0048T^2 + 0.881T + 8.5714$
$R^2 = 0.9995$

Fig. 9. Accumulated infiltration and the obtained equation using 30 cm diameter single infiltrometer

Table 9. Soil texture analysis, [15], in two different sites

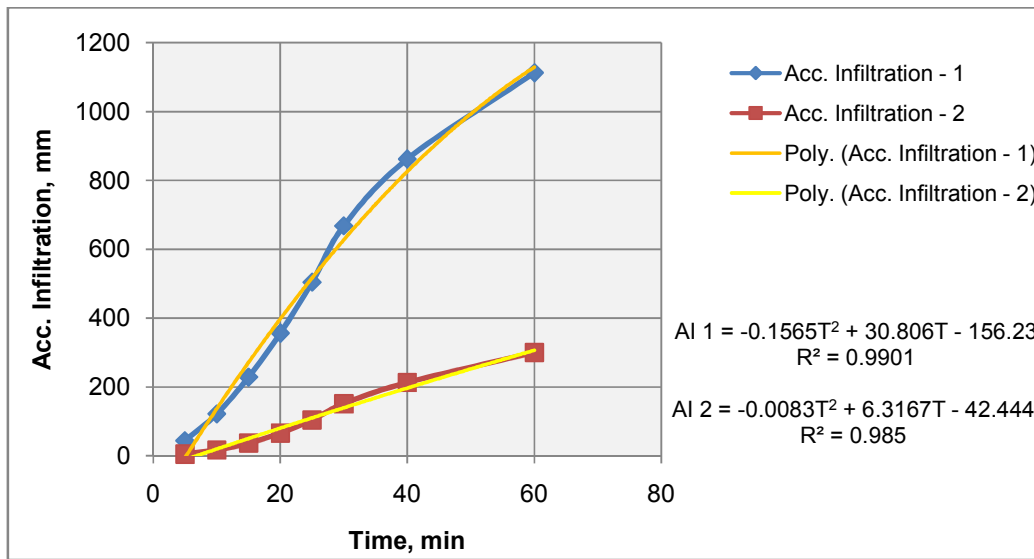| Depth, cm	Site 1	Site 2
0 – 30	Sandy clay	Sandy clay
30 – 60	Sandy clay	Clay

Experimental infiltration measurements are performed at four different locations with various farming lands, [16], using a double ring infiltrometer. Soil texture analyses and land covers are shown in table 11. The raw data for the accumulated infiltration are presented in table 12. Excel approach is applied on the raw infiltration data, where Figs. 11 and 12 illustrate the accumulated infiltration versus the time, the polynomial regression, and the obtained equations with very high R^2.

Experimental infiltration measurements are performed at four different locations with various farming lands, [17], using a double ring infiltrometer. Soil texture analyses and land

covers are shown in Table 13. The raw data for the accumulated infiltration are presented in Table 14. Excel approach is applied on the raw infiltration data, where Figs. 13 and 14 illustrate the accumulated infiltration versus the time, the polynomial regression, and the obtained equations with very high R^2.

Table 10. Raw measurements, [15], for infiltration in two sites with different soil textures

Site	Site 1	Site 2
Time, min	Acc. Infiltration - 1, mm	Acc. Infiltration - 2, mm
5	44	05
10	122	17
15	228	37
20	356	66
25	504	104
30	668	151
40	862	213
60	1112	300

AI 1 = -0.1565T² + 30.806T - 156.23
R² = 0.9901

AI 2 = -0.0083T² + 6.3167T - 42.444
R² = 0.985

$AI\ 1 = -0.1565T^2 + 30.806T - 156.23$
$R^2 = 0.9901$

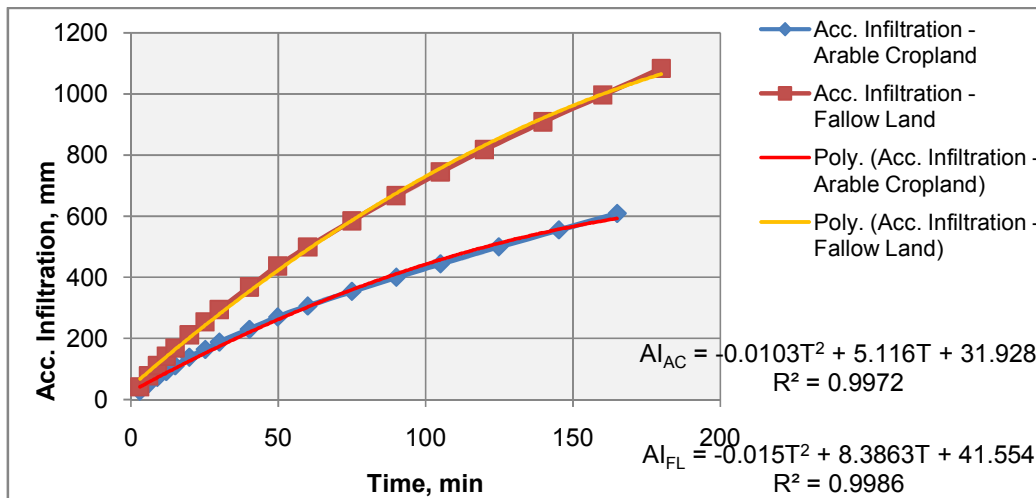$AI\ 2 = -0.0083T^2 + 6.3167T - 42.444$
$R^2 = 0.985$

Fig. 10. Accumulated infiltration and the obtained equation in two sites with different soil textures

Table 11. Soil texture analysis, [16], and land covers for various farming lands

Soil analyses	Land cover			
	Arable cropland	Fallow land	Cultivated land	Pineapple farm
% Sand	83	83	81	81
% Silt	2	2	1	2
% Clay	15	15	18	17
Soil Texture	Sandy Loam	Sandy Loam	Sandy Loam	Sandy Loam

Table 12. Raw measurements, [16], for infiltration in four different locations with various farming lands

Time, min	Acc. infiltration - arable cropland, mm	Acc. infiltration - fallow land, mm	Acc. infiltration - cultivated land, mm	Acc. infiltration - pineapple farm, mm
3	28	41	27	36
6	52	77	52	68
9	73	111	74	97
12	92	141	94	123
15	110	168	112	147
20	139	211	138	184
25	164	254	164	218
30	188	294	189	250
40	230	368	235	311
50	270	437	280	369
60	306	499	324	423
75	354	585	388	493
90	400	667	451	556
105	444	745	515	615
120	---	818	574	665
125	500	---	---	---
140	---	909	653	730
145	555	---	---	---
160	---	997	730	793
165	609	---	---	---
180	---	1084	807	856

$$AI_{AC} = -0.0103T^2 + 5.116T + 31.928$$
$$R^2 = 0.9972$$

$$AI_{FL} = -0.015T^2 + 8.3863T + 41.554$$
$$R^2 = 0.9986$$

Fig. 11. Accumulated infiltration and the obtained equations for two land covers

Table 13. Soil texture analysis, [17], and land covers for various farming lands

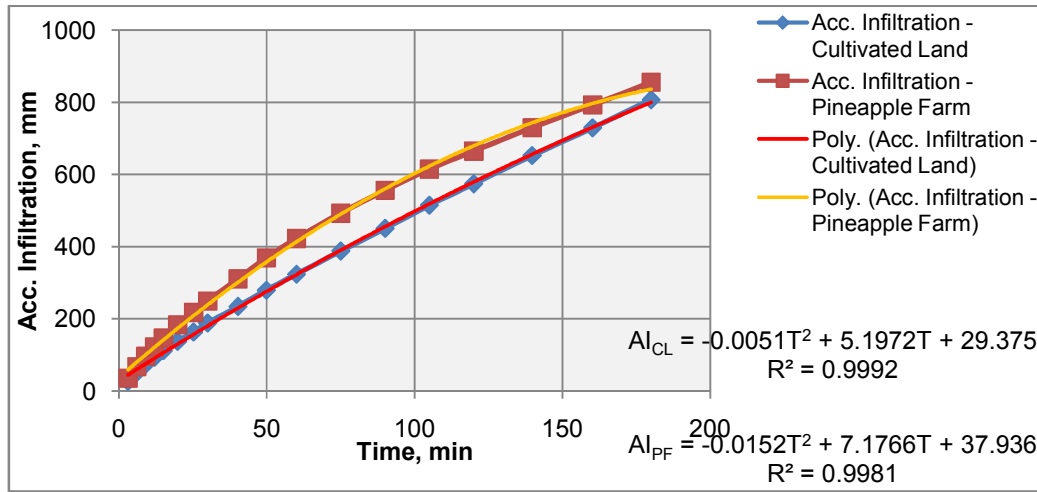| Soil analyses	Land cover			
	Grazing land	Secondary forest	Cultivated land	Plantain plantation
% Sand	77	72	83	83
% Silt	7	12	9	11
% Clay	16	16	8	6
Soil Texture	Sandy Loam	Sandy Loam	Loamy Sand	Loamy Sand

Fig. 12. Accumulated infiltration and the obtained equations for other land covers

Table 14. Raw measurements, [17], for infiltration in four different locations with various farming lands

Time, min	Acc. infiltration - grazing land, mm	Acc. infiltration – secondary forest, mm	Acc. infiltration - cultivated land, mm	Acc. infiltration – plantain plantation, mm
2	3.4	4.1	3.0	4.2
4	7.3	8.4	6.1	8.8
7	11.6	13.5	9.7	14.2
10	16.1	19.1	13.2	19.4
15	22.1	25.8	17.5	26.0
20	27.8	32.6	22.0	33.1
25	33.6	40.0	26.5	40.1
30	39.5	48.0	31.2	47.2
40	46.5	61.0	43.2	58.1
50	53.9	74.6	47.3	69.6
65	63.7	89.9	58.9	82.8
80	73.9	107.0	71.3	95.8
100	86.3	125.1	85.6	110.3
120	98.8	141.4	100.0	125.0
150	112.9	159.8	115.8	141.8
180	127.3	178.5	131.8	158.7

It is concluded from the last figures 3 through 14 that the Excel approach introduces a polynomial infiltration model, which has a very high accuracy representing the accumulated infiltration versus the time. The Polynomial infiltration model of Excel approach can be expressed in general formula as in equation 1.

$$AI = A\,T^2 + B\,T + C \qquad (1)$$

Where: AI = Accumulated infiltration (mm),
T = Time from start (min),
A, B and C = Constants according to specific conditions.

3.2 Validation of Polynomial Infiltration Model

In order to test the predictive power of the Polynomial infiltration model, the derived equations are to be validated. The gathered data are divided into calibration and validation groups with ratios of 80% and 20% respectively, [18]. Validation check is performed as shown in Fig. 15. The observed accumulated infiltration represents the values of the experimental infiltration measurements, while the predicted accumulated infiltration represents the obtained values employing the Polynomial infiltration
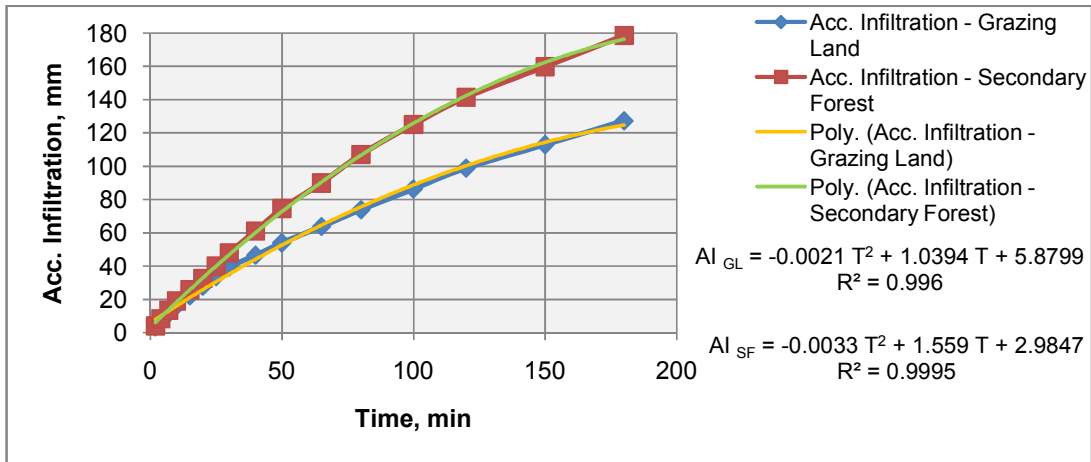
Fig. 13. Accumulated infiltration and the obtained equations for two land covers
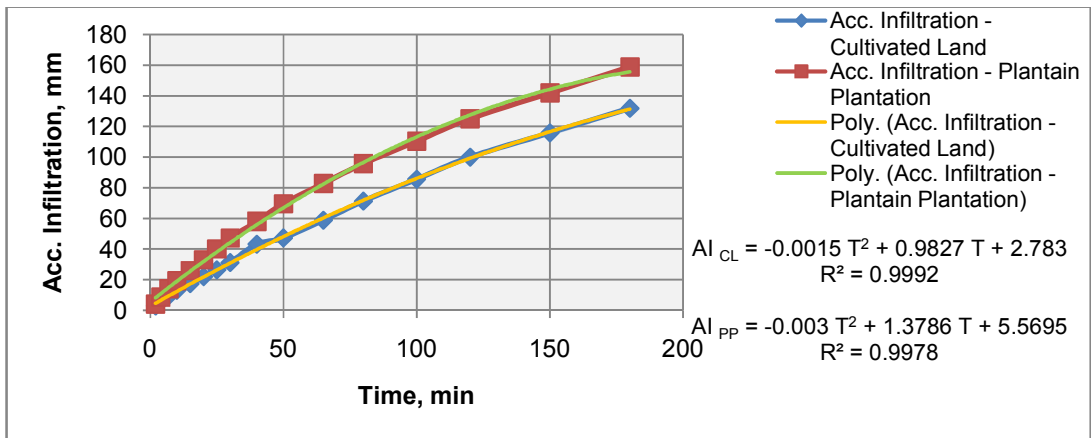
$AI_{GL} = -0.0021\ T^2 + 1.0394\ T + 5.8799$
$R^2 = 0.996$

$AI_{SF} = -0.0033\ T^2 + 1.559\ T + 2.9847$
$R^2 = 0.9995$

Fig. 14. Accumulated infiltration and the obtained equations for other land covers

$AI_{CL} = -0.0015\ T^2 + 0.9827\ T + 2.783$
$R^2 = 0.9992$

$AI_{PP} = -0.003\ T^2 + 1.3786\ T + 5.5695$
$R^2 = 0.9978$
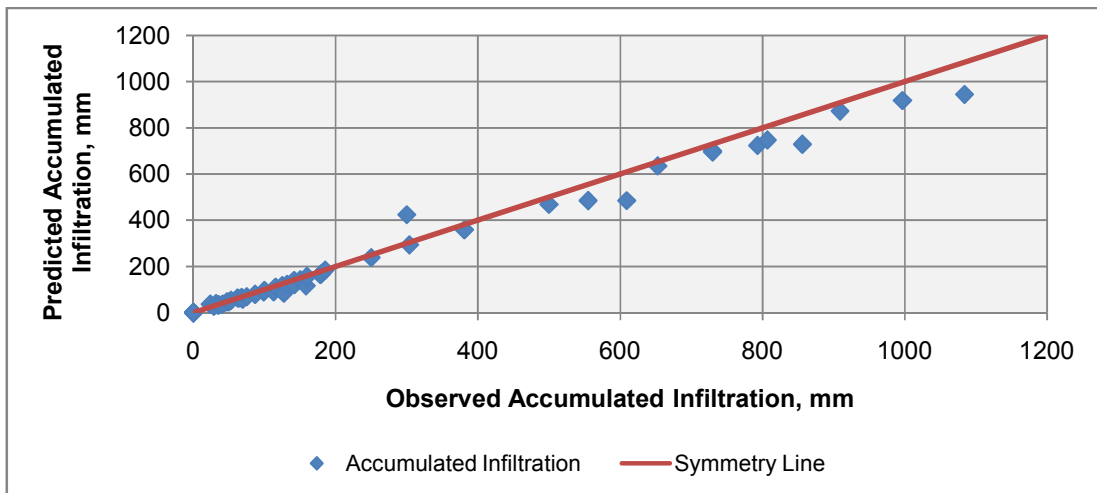
Fig. 15. Validation check for the Polynomial infiltration model

equations. On the symmetry line, the predicted infiltration is equal to the observed infiltration, which means 100% accuracy. Due to the very high accuracy of the Polynomial infiltration model, all the points lie very close to the symmetry line.

3.3 Analyses Employing Horton and Kostiakov Infiltration Models

To simplify the infiltration processes, several equations are developed for field applications. These empirical models relate infiltration rate or volume to elapsed time according to certain properties. Parameters used in these models can be estimated from measured infiltration - time relationships for a given soil condition. The empirical infiltration models include the two widely used Horton and Kostiakov models.

Horton infiltration model, [13], expresses the relation of infiltration capacity with time as an exponential function, as shown in equation 2.

$$f = f_c + (f_o - f_c) e^{-kt} \qquad (2)$$

Where: f = infiltration capacity at any time t,
f_c = final steady state infiltration capacity,
f_o = initial infiltration capacity,
k = Horton's constant representing rate of decrease in infiltration capacity,
t = time.

Kostiakov infiltration model, [13], presents a simple power function relating the infiltration with the time t, as shown in equation 3.

$$f = a\, t^{\alpha} \qquad (3)$$

Where: f = accumulated infiltration at any time t,
t = time,
(a) and (α) are constants.

All the gathered thirty one raw experimental infiltration measurements are analyzed employing both Horton and Kostiakov infiltration models. The values of different constants of Horton (k) and Kostiakov (a and α) infiltration models and their coefficient of determination (R^2) for all cases are obtained, as illustrated in Table 15. Also, Table 15 includes R^2 associated with the Polynomial infiltration model of Excel approach.

From the results in Table 15, it is found that the polynomial infiltration model of Excel approach has higher accuracy, followed by Kostiakov infiltration model, and finally Horton infiltration

model. The polynomial infiltration model of Excel approach has an average value of R^2 of 0.9967, where the values of R^2 range between 0.9850 and 0.9998. Kostiakov infiltration model has an average value of R^2 of 0.9906, where the values of R^2 range between 0.9651 and 0.9993. Finally, Horton infiltration model has an average value of R^2 of 0.8467, where the values of R^2 range between 0.6907 and 0.9805.

It is noted that there is only one case where Horton infiltration model has more accuracy than Kostiakov infiltration model. This case concerns experiment 5 shown in Fig. 8. The reason may be due to inaccurate infiltration measurements, which are performed using a single infiltrometer. For this specific case, the polynomial infiltration model of Excel approach is still having higher accuracy.

The developed polynomial infiltration model describes very well all the experimental results within their associated time values. Attention has to be paid when concerning very low or very high time values, which are not employed in the experiment. Employing very low time values in the obtained equations may give false results (negative values) for the expected accumulated infiltration, such as case A3 in Fig. 5 that gives negative value for time of 1 min. The very high time values may be employed in the obtained equations only when the basic infiltration rate is not known, [6]. If the basic infiltration rate is known, then its value is added to predict the accumulated infiltration. If the basic infiltration rate is not known, the obtained equations are used carefully to avoid false results for the expected accumulated infiltration.

3.4 Types of Land Cover and Soil Texture for Polynomial, Horton and Kostiakov Infiltration Models

Considering the land cover, it is noted that the gathered raw experimental infiltration measurements can be categorized into three main types, as illustrated in Table 16. These types are bare land, forest land and irrigated land. It has to be noted that the land cover for the two experimental measurements represented in Fig. 10 are not defined.

Table 16 includes the average values for the coefficient of determination (R^2) for the Polynomial, Horton and Kostiakov infiltration models according to the land cover type. For all land cover types, the Polynomial infiltration

Table 15. Analyses of infiltration measurements employing Excel approach, Horton, and Kostiakov infiltration models

Case of accumulated infiltration	Polynomial model (Excel approach)	Exponential model (Horton equation)		Power model (Kostiakov equation)		
	R^2	k	R^2	a	α	R^2
Figure 3	0.9979	0.0333	0.7573	5.3206	0.6570	0.9912
Figure 4	0.9988	0.3536	0.8869	15.6810	0.9512	0.9846
Figure 5, A1	0.9948	0.0303	0.9176	10.2570	0.3930	0.9955
Figure 5, A2	0.9861	0.0248	0.8374	14.6390	0.3307	0.9651
Figure 5, A3	0.9958	0.0541	0.8433	8.0339	0.7216	0.9685
Figure 5, A4	0.9971	0.0280	0.8986	15.8010	0.3653	0.9901
Figure 5, A5	0.9964	0.0567	0.8818	8.2933	0.7452	0.9846
Figure 6, B1	0.9987	0.0432	0.8724	19.9910	0.7258	0.9914
Figure 6, B2	0.9991	0.0391	0.9039	30.9240	0.6487	0.9982
Figure 6, B3	0.9996	0.0413	0.9358	16.7430	0.6735	0.9993
Figure 6, B4	0.9968	0.0378	0.8520	19.4940	0.6413	0.9849
Figure 6, B5	0.9967	0.0419	0.8608	32.5460	0.7071	0.9875
Figure 7, AI1	0.9983	0.0244	0.8760	7.8515	0.7331	0.9886
Figure 7, AI2	0.9993	0.0220	0.9341	4.5577	0.6413	0.9992
Figure 7, AI3	0.9958	0.0174	0.8725	5.0249	0.5220	0.9875
Figure 8, AI4	0.9961	0.0128	0.8955	5.6979	0.4248	0.9947
Figure 8, AI5	0.9976	0.0104	0.9805	5.8504	0.3264	0.9748
Figure 8, AI6	0.9980	0.0169	0.9002	3.8234	0.5023	0.9934
Figure 9, AI7	0.9957	0.0232	0.9453	2.0771	0.6721	0.9956
Figure 9, AI8	0.9998	0.0211	0.9626	4.3522	0.6046	0.9960
Figure 9, AI9	0.9995	0.0162	0.9139	4.9529	0.5347	0.9977
Figure 10, AI1	0.9901	0.0536	0.7708	5.5437	1.3611	0.9829
Figure 10, AI2	0.9850	0.0688	0.7869	0.3393	1.7327	0.9862
Figure 11, AI$_{AC}$	0.9972	0.0151	0.7673	13.8910	0.7503	0.9971
Figure 11, AI$_{FL}$	0.9986	0.0147	0.8013	19.4030	0.7860	0.9991
Figure 12, AI$_{CL}$	0.9992	0.0154	0.8013	12.0960	0.8073	0.9991
Figure 12, AI$_{PF}$	0.9981	0.0141	0.7582	18.0450	0.7592	0.9962
Figure 13, AI$_{GL}$	0.9960	0.0156	0.6907	2.5024	0.7772	0.9925
Figure 13, AI$_{SF}$	0.9995	0.0170	0.7094	2.6315	0.8370	0.9967
Figure 14, AI$_{CL}$	0.9992	0.0172	0.7401	1.8582	0.8302	0.9986
Figure 14, AI$_{PP}$	0.9978	0.0159	0.6958	2.9510	0.7914	0.9945
Average R^2	**0.9967**		**0.8467**		**0.9906**	

model has higher accuracy, followed by Kostiakov infiltration model, and finally Horton infiltration model.

For Polynomial infiltration model, the higher average R^2 is associated with the forest land followed by the irrigated land and the bare land. The values of R^2 are 0.9978, 0.9977 and 0.9961 respectively. For Horton infiltration model, the higher average R^2 is associated with the forest land followed by the bare land and the irrigated land. The values of R^2 are 0.9201, 0.8731 and 0.7923 respectively. For Kostiakov infiltration model, the higher average R^2 is associated with the irrigated land followed by the forest land and the bare land. The values of R^2 are 0.9921, 0.9919 and 0.9882 respectively.

Studying the types of soil texture, it is found that the gathered raw experimental infiltration measurements can be categorized into four main types, as illustrated in Table 17. These types are loam, sandy clay loam, sandy loam and loamy sand. It has to be noted that the soil texture for the three experimental measurements represented in Figs. 7, 8 and 9 are not defined.

Table 17 includes the average values for the coefficient of determination (R^2) for the Polynomial, Horton and Kostiakov infiltration models according to both soil texture and land cover types. For all cases, the Polynomial infiltration model has higher accuracy, followed by Kostiakov infiltration model, and finally Horton infiltration model.

Table 16. Types of land cover for gathered infiltration experimental measurements with average R^2 for the Polynomial, Horton and Kostiakov infiltration models

Case of accumulated infiltration	Land cover	Polynomial Av R^2	Horton Av R^2	Kostiakov Av R^2
Figure 5, A1	Bare land	0.9961	0.8731	0.9882
Figure 5, A2				
Figure 5, A3				
Figure 6, B1				
Figure 6, B2				
Figure 6, B3				
Figure 11, AI$_{FL}$				
Figure 7, AI1	Forest land	0.9978	0.9201	0.9919
Figure 7, AI2				
Figure 7, AI3				
Figure 8, AI4				
Figure 8, AI5				
Figure 8, AI6				
Figure 9, AI7				
Figure 9, AI8				
Figure 9, AI9				
Figure 3	Irrigated land	0.9977	0.7923	0.9921
Figure 4				
Figure 5, A4				
Figure 5, A5				
Figure 6, B4				
Figure 6, B5				
Figure 11, AI$_{AC}$				
Figure 12, AI$_{CL}$				
Figure 12, AI$_{PF}$				
Figure 13, AI$_{GL}$				
Figure 13, AI$_{SF}$				
Figure 14, AI$_{CL}$				
Figure 14, AI$_{PP}$				

For loam soil, there is only one land cover, which is the irrigated land.

For sandy clay loam soil, the higher average R^2 is associated with the irrigated land followed by the bare land for the three infiltration models.

For sandy loam soil, the higher average R^2 is associated with the irrigated land followed by the bare land for Polynomial and Kostiakov infiltration models, while the higher average R^2 is associated with the bare land followed by the irrigated land for Horton infiltration model.

For loamy sand soil, the higher average R^2 is associated with the bare land followed by the irrigated land for the three infiltration models.

3.5 Effect of Soil Texture and Land Cover on the Polynomial Infiltration Model of Excel Approach

Other analyses are performed to study the effect of both soil texture and land cover on the polynomial infiltration model of Excel approach. The constants A, B and C of the obtained equation of the polynomial infiltration model, equation 1, are considered according to specific conditions.

Investigating the obtained equations in case of forest land cover, as illustrated in Table 16, it is found that the values of A range between -0.025 and -0.001, the values of B range between 0.24 and 3.89, and the values of C range between 3.5

and 10.6. It has to be noted that the soil textures for these nine cases are not defined.

For the rest twenty-two cases, as shown in Table 17, considering the effect of soil texture on the constant A, it is found that all values are negative. The values of A range between -0.195 and -0.002 for sandy loam soil, between -0.111 and -0.001 for loamy sand soil, between -0.103 and -0.018 for loam soil, between -1.329 and -0.120 for sandy clay loam soil, and between -0.008 and -0.156 for sandy clay soil. There is no specific trend for the effect of the associated land cover.

Similarly, considering the effect of soil texture on the constant B, it is found that all values are positive. The values of B range between 1.03 and 17.03 for sandy loam soil, between 0.98 and 11.56 for loamy sand soil, between 2.15 and 8.28 for loam soil, between 6.12 and 21.14 for sandy clay loam soil, and between 6.31 and 30.80 for sandy clay soil. There is no specific trend for the effect of the associated land cover except for loamy sand soil, where B values in case of bare land are greater than B values in case of irrigated land.

Finally, considering the effect of soil texture on the constant C, it is found that all values are positive except for sandy clay and sandy clay loam soils. That may be due to the increase of clay content in these soils. The values of C range between -5.02 and -3.60 for sandy clay loam soil, and between -156.20 and -42.40 for sandy clay soil, with no specific trend for the effect of the associated land cover. The values of C range between 1.40 and 41.55 for sandy loam soil, between 4.88 and 14.71 for loam soil, with no specific trend for the effect of the associated land cover. The values of C range between 2.78 and 32.85 for loamy sand soil, with C values in case of bare land are greater than C values in case of irrigated land.

In fact, many factors affect infiltration such as moisture content, soil texture and structure, porosity and permeability, soil bulk density and compaction, vegetative cover, root depth and organic content, slope, and topography. For each specific location, the infiltration depends on some parameters that are commonly got from various measurements.

One or some of the infiltration models are better and appropriate for a specific site, [19], where Horton's model was better than the Kostiakov-Lewis and Philip's models at most sample points in the studied area. Another study was conducted

Table 17. Types of soil texture and land cover for gathered infiltration experimental measurements with average R^2 for the Polynomial, Horton and Kostiakov infiltration models

Case of accumulated infiltration	Soil texture	Land cover	Polynomial Av R^2	Horton Av R^2	Kostiakov Av R^2
Figure 3 Figure 6, B4	Loam	Irrigated land	0.9974	0.8047	0.9881
Figure 5, A3	Sandy Clay	Bare land	0.9958	0.8433	0.9685
Figure 4	Loam	Irrigated land	0.9988	0.8869	0.9846
Figure 5, A1 Figure 5, A2 Figure 6, B1 Figure 11, AI$_{FL}$	Sandy Loam	Bare land	0.9946	0.8572	0.9878
Figure 5, A4 Figure 5, A5 Figure 6, B5 Figure 11, AI$_{AC}$ Figure 12, AI$_{CL}$ Figure 12, AI$_{PF}$ Figure 13, AI$_{GL}$ Figure 13, AI$_{SF}$		Irrigated land	0.9975	0.7960	0.9930
Figure 6, B2 Figure 6, B3	Loamy Sand	Bare land	0.9994	0.9199	0.9988
Figure 14, AI$_{CL}$ Figure 14, AI$_{PP}$		Irrigated land	0.9985	0.7180	0.9966

to evaluate Philip and Kostiakov infiltration models on three different soils, [20]. Philip model gave the best prediction of water infiltration in coastal plain sands soil, while the Kostiakov model was best for soils of sandstone and river alluvium. It is noted that this study concerned only with investigating the effect of soil texture on the infiltration, and neglected the effect of other factors such as moisture content, land cover, slope and topography. However, infiltration models have to be tested for the ability to estimate the infiltration of each location and it has to be documented at each site.

4. CONCLUSIONS

It is concluded that the presented polynomial infiltration model of Excel approach for the accumulated infiltration is associated with high accuracy, where the values of coefficient of determination (R^2) range between 0.9850 and 0.9998. The obtained equations can help in irrigation processes. It is possible to determine how long it will take to infiltrate a certain amount of water, which is important for irrigation purposes.

It is found that the polynomial infiltration model of Excel approach has higher accuracy, followed by Kostiakov infiltration model, and finally Horton infiltration model.

Considering types of land cover, the descending average R^2 is associated with the forest land, the irrigated land, and the bare land for Polynomial infiltration model. For Horton infiltration model, the descending average R^2 is associated with the forest land, the bare land, and the irrigated land. For Kostiakov infiltration model, the descending average R^2 is associated with the irrigated land, the forest land, and the bare land.

Studying the types of both soil texture and land cover, the higher average R^2 is associated with the irrigated land followed by the bare land for the three infiltration models for sandy clay loam soil. For loamy sand soil, the higher average R^2 is associated with the bare land followed by the irrigated land for the three infiltration models. For sandy loam soil, the higher average R^2 is associated with the irrigated land followed by the bare land for Polynomial and Kostiakov infiltration models, while the higher average R^2 is associated with the bare land followed by the irrigated land for Horton infiltration model.

Analyses are performed to study the effect of both soil texture and land cover on the constants

A, B and C of the obtained equation of the polynomial infiltration model of Excel approach. It is found that all constant A values are negative, all constant B values are positive, and all constant C values are positive except for sandy clay and sandy clay loam soils. There is no specific trend for the effect of the associated land cover on constant A values. For constants B and C, there is no specific trend for the effect of the associated land cover except for loamy sand soil, where B and C values in case of bare land are greater than their values in case of irrigated land.

However, infiltration models have to be tested for the ability to estimate the infiltration of each location, and it has to be documented at each site.

COMPETING INTERESTS

Author has declared that no competing interests exist.

REFERENCES

1. Green W. Heber, Ampt GA. Studies on soil physics. The Journal of Agricultural Science. 1911;4:1. DOI:10.1017/S0021859600001441
2. Water Resources Engineering, Edition, John Wiley & Sons, Inc; 2005.
3. Horton Robert E. The role of infiltration in the hydrologic cycle. Trans. Am. Geophys. Union. 14th Ann. Mtg. 1933;446–460. Bibcode: 1933TrAGU.14..446H. DOI:10.1029/TR014i001p00446.
4. Kostiakov AN. On the dynamics of the coefficient of water-percolation in soils and on the necessity of studying it from a dynamic point of view for purposes of amelioration. Transactions of 6th Congress of International Soil Science Society. Moscow. pp. 17–21
5. Walker WR, Skogerboe GV. Surface irrigation: Theory and practice. Prentice-Hall, Englewood Cliffs; 1987.
6. Available:http://www.fao.org/docrep/S8684E/s8684e0a.htm
7. Available:https://player.slideplayer.com/72/12283235/slides/slide_20.jpg
8. Available:www.slideserve.com/naida-charles/6346611
9. Angulo-Jaramillo R, Bagarello V, Iovino M, Lassabatere L. Saturated soil hydraulic conductivity. In: Infiltration Measurements for Soil Hydraulic Characterization. Springer, Cham; 2016.

10. Wang X, Amonett C, Williams JR, Wilcox BP, Fox WE, Tu MC. Rangeland watershed study using APEX. J. Soil Water Conserv. 2014;69(3):197-212. DOI:10.2489/jswc.69.3.197

11. Tu MC, Smith P. Modelling pollutant buildup and washoff parameters for SWMM based on land use in a semiarid urban watershed. Water Air Soil Poll. 2018;229:121. DOI:10.1007/s11270-018-3777-2

12. Alatise MO, Akinola FF. Prediction of infiltration capacities by field measurement and selected empirical models for irrigated agriculture. Archives of Current Research International. 2017;9(1): 1-10.

13. Patil VS, Chavan SM, Pawar DP. Spatial distribution of soil under the influence of infiltration rate. Journal of Pharmacognosy and Phytochemistry. 2018;7(2):2024-2029

14. Patra KC, Kumar BV. Determination of infiltration rate of soils using single and double ring infiltrometer and study of drought analysis in Karimnagar District of Andhra Pradesh. Department of Civil Engineering, National Institute of Technology, Rourkela Odisha – 769008, India; 2014.
Available:www.ethesis.nitrkl.ac.in/6051/1/110CE0357-11.pdf

15. Folorunso OP, Aribisala JO. Effect of soil texture on soil infiltration rate. Archives of Current Research International. 2018; 14(3):1-8.

16. Osuji GE, Okon MA, Chukwuma MC, Nwarie II. Infiltration characteristics of soil under selected land use practices in Owerri, Southeastern Nigeria. Nwarie World Journal of Agriculture Sciences. 2010;6(3):322-326.

17. Onyegbule UO, Azu Donatus EO, Akagha UN. Infiltration characteristics of soils in Owerri, Imo State, Southeastern Nigeria under four selected land uses. Asian Soil Research Journal. 2018;1(3):1-8.

18. Tu MC, Smith P, Filippi AM. Hybrid forward-selection method-based water-quality estimation via combining Landsat TM, ETM+, and OLI/TIRS images and ancillary environmental data. PLoS ONE. 2018;13(7):e0201255. DOI:10.1371/journal.pone.0201255

19. Haghighi FM, Gorji M, Shorafa F, Sarmadian, Mohammadi MH. Evaluation of some infiltration models and hydraulic parameters. Spanish Journal of Agricultural Research. 2010;8(1):210-217.

20. Utin UE, Oguike PC. Evaluation of Philip's and Kostiakov's infiltration models on soils derived from three parent materials in Akwa Ibom State, Nigeria. Journal of Scientific and Engineering Research. 2018;5(6):79-87.